Rational Design and Direct Fabrication of Multi-walled hollow electrospun fibers with Controllable Structure and Surface Properties

Jamal Seyyed Monfared Zanjani, Burcu Saner Okan, Ilse Letofsky-Papst, Mehmet Yildiz, Yusuf Menceloglu

PII: S0014-3057(14)00371-1
DOI: http://dx.doi.org/10.1016/j.eurpolymj.2014.10.019
Reference: EPJ 6603

To appear in: *European Polymer Journal*

Received Date: 27 July 2014
Revised Date: 15 October 2014
Accepted Date: 26 October 2014

Please cite this article as: Zanjani, J.S.M., Okan, B.S., Letofsky-Papst, I., Yildiz, M., Menceloglu, Y., Rational Design and Direct Fabrication of Multi-walled hollow electrospun fibers with Controllable Structure and Surface Properties, *European Polymer Journal* (2014), doi: http://dx.doi.org/10.1016/j.eurpolymj.2014.10.019

Rational Design and Direct Fabrication of Multi-walled hollow electrospun fibers with Controllable Structure and Surface Properties

Jamal Seyyed Monfared Zanjani[1], Burcu Saner Okan[2], Ilse Letofsky-Papst[3], Mehmet Yildiz[1] and Yusuf Menceloglu[1]

[1]Faculty of Engineering and Natural Sciences, Sabanci University, Tuzla, Istanbul 34956, Turkey
[2]Sabanci University Nanotechnology Research and Application Center, SUNUM, Tuzla, Istanbul 34956, Turkey
[3]Institute for Electron Microscopy, Graz University of Technology, Steyrergasse 17, A-8010, Graz, Austria

Keywords: Composites, core-shell structures, hollow fibers, multilayers, tri-axial electrospinning

Abstract

Multi-walled hollow fibers with a novel architecture are fabricated through utilizing a direct, one-step tri-axial electrospinning process with a manufacturing methodology which does not require any post-treatments for the removal of core material for creating hollowness in the fiber structure. The hydrophilicity of both inner and outer layers' solution needs to be dissimilar and carefully controlled for creating a two-walled/layered hollow fiber structure with a sharp interface. To this end, Hansen solubility parameters are used as an index of layer solution affinity hence allowing for control of diffusion across the layers and the surface porosity whereby an ideal multi-walled hollow electrospun fiber is shown to be producible by tri-axial electrospinning process. Multi-walled hollow electrospun fibers with different inner and outer diameters and different surface morphology are successfully produced by using dissimilar material combinations for inner and outer layers (i.e., hydrophobic polymers as outer layer and hydrophilic polymer as inner layer). Upon using different material combinations for inner and outer layers, it is shown that one may control both the outer and inner diameters of the fiber. The inner layer not only acts as a barrier and thus provides an ease in the encapsulation of functional core materials of interest with different viscosities but also adds stiffness to the fiber. The structure and the surface morphology of fibers are controlled by changing applied voltage, polymer types, polymer concentration, and the evaporation rate of solvents. It is demonstrated that if the vapor pressure of the solvent for a given outer layer polymer is low, the fiber diameter decreases down to 100 nm whereas solvents with higher vapor pressure result in fibers with the outer diameter of up to 1 μm. The influence of electric field strength on the shape of Taylor cone is also monitored during the production process and the manufactured fibers are structurally investigated by relevant surface characterization techniques.

1. Introduction

Hollow structured nanofibers with exceptional properties such as low density, high specific surface area, and tunable surface properties have found considerable applications in catalysis [1], drug delivery [2], membrane [3], and photonics [4]. Up to now, two different approaches have been developed to fabricate hollow fibers through electrospinning process. The first approach introduced by Bognitzki et al. [5] uses the conventional electrospun polymeric fibers as templates for the fabrication of hollow fibers through coating the templates with wall materials using various deposition techniques, and then removes the template to obtain hollow structures. Similar procedure was utilized in the fabrication of hollow fibers of titanium dioxide [6], silica [7] and alumina [8]. Complexity in coating, template removal

processes and type of material are the limiting factors of the method in question for the production of hollow fibers. The second approach employs co-axial electrospinning process to produce core-shell fibers from two different solutions and then hollow structured fibers is fabricated by selective removal of the core material. Li et al. [9, 10] used co-electrospinning of polyvinylpyrrolidone and titanium tetraisopropoxide solution in ethanol as the shell and mineral oil as the core, which is followed by the subsequent extraction of oil and calcination process to fabricate hollow titania fibers. In another study, hollow carbon nanotubes were fabricated by co-electrospinning of poly(methyl methacrylate) (PMMA) solution as fiber's core and polyacrylonitrile (PAN) as fiber's shell with the subsequent degradation of PMMA and then carbonization of PAN [11]. Dror et al. [12] fabricated polymeric bio-microtubes by using co-electrospun biocompatible and biodegradable polymers as core and shell of fibers and transformed the core/shell structure into hollow fibers by controlling the evaporation of the core solution.

In order to increase the strength and functionality of co-axial electrospun fibers, an additional wall in fiber structure is provided by multi-axial electrospinning which is a single-step method to fabricate third generation electrospun nanofibers with a unique architecture and morphology. In the fabrication process of multi-axial electrospun nanofibers, a strong electric field is applied between a nozzle containing concentric tubes allowing for the extrusion of different fluids to tip of the nozzle and grounded metallic plate as a collector. When the electrostatic forces on the surface of polymeric solutions exceed the surface tension of droplets, the jet of polymeric solutions is ejected from the tip of the nozzle and undergoes bending instabilities, whipping motions and diameter reduction in order to form multi-axial fibers with diameter ranging from several nanometers to micrometers [13]. The advantage of these sandwich-structured fibers is in the insertion of an extra intermediate layer between the inner cavity and outer wall of fibers. This extra layer would provide an inert medium for the core material to be encapsulated thereby reducing the environmental effect and increasing the life time of both core and wall materials.

In literature, one may find a few recent studies which have utilized tri-axial electrospinning technique that focuses on the encapsulation of functional molecules since an extra intermediate layer in electrospun fiber increases the life time of encapsulated materials. Kalra et al. [14] applied tri-axial electrospinning technique to produce fibers with intermediate layer of block-copolymers with self-assembly functionality flanked between the shell layers of thermally stable silica and the core allowing for the post-fabrication annealing of the fibers to obtain equilibrium self-assembly without destroying the fibers morphology. In another study, tri-axial electrospinning technique was utilized to develop nanowire-in-microtube structure by introducing an extra middle fluid as a spacer between the outer and inner layer of fibers and selective removing of middle spacer fluid to achieve hollow cavity between the sheath and the core materials [15]. In another work, biodegradable triaxial nanofibers were produced by using gelatin as middle wall and poly(ε-caprolactone) as inner and outer walls to provide sufficient strength to support developing tissues [16]. Especially these types of multi-axial electrospun fibers have been utilized as drug delivery vehicles since the structure of fiber provides a quick release from the outer sheath layer for short-term treatment and a sustained release from the fiber core for long-term treatment [17].

This study differs from the previous studies in terms of creating hollow and continuous triaxial electrospun fibers in a single step without any post treatments in which hollowness can be tailored. Having a two-walled structure strengthens the electrospun fibers thereby preventing its deformation and in turn leading to continuous fiber structure. Herein, the

hollowness of tri-axial electrospun fibers with different outer and inner diameters is controlled by using several solvent-polymer systems and different layer polymers to increase encapsulation efficiency. Hansen solubility parameters are applied to get an index of layer solution miscibility and affinity to control the diffusion of layers through multi-axial electrospinning. To our best knowledge, the current study is the first one for the production of multi-walled hollow fibers by a single-step process without applying any post treatments and inserting any spacer through layers. In this process, two spinnable polymer solutions as inner and outer layers of fibers with different polarities and viscosities adjusted by changing polymer concentration are chosen to provide composite properties and wider range of applications. In place of multi-axial electrospinning process, single electrospinning methodology is also applied to optimize solution concentration to get well-ordered fiber structure. The diameter, surface morphology and layered structure of multi-walled hollow electrospun fibers are controlled by tailoring the solvent properties, degree of miscibility of solutions, polymer concentration, applied voltage, electrospinning distance, and flow rate.

2. Experimental

2.1. Materials

The following materials have been used for the experiment: Methyl methacrylate (SAFC, 98.5%), styrene (SAFC, 99%), Azobisisobutyronitrile (AIBN, Fluka, 98%), acrylamide (Sigma, 99%), N, N dimethyl formamide (DMF, Sigma-Aldrich, 99%), methanol (Sigma-Aldrich, 99.7%), tetrahydrofuran (THF, Merck, 99%), ethyl acetate (EA, Sigma-Aldrich, 99.5%).

2.2. Layer material synthesis

Polymethyl methacrylate (PMMA), polystyrene (PS) and poly(methyl methacrylate-co-styrene) as hydrophobic polymers and outer layer materials of fibers were synthesized by free radical polymerization of vinyl monomers (30 ml) in presence of AIBN (1 g) as the radical initiator in the medium of THF (50 ml) at 65°C. Polymerization reaction was carried out for 4 h and then the reaction mixture was precipitated in cold methanol and dried for 12 h in a vacuum oven at 50°C. Polyacrylamide (PAAm) as hydrophilic polymer and inner layer material was synthesized by dispersion polymerization of acrylamide monomer (30 g) in methanol (100 ml) by using AIBN (1 g) as an initiator at 65°C. Separation of polymer particles from methanol and monomer mixture was done by vacuum filtration and twice washing the polymer particles with methanol and drying it for 12 h in a vacuum oven at 40°C. Figure 1 represents the chemical structures of layer materials chosen for multi-axial electrospinning process.

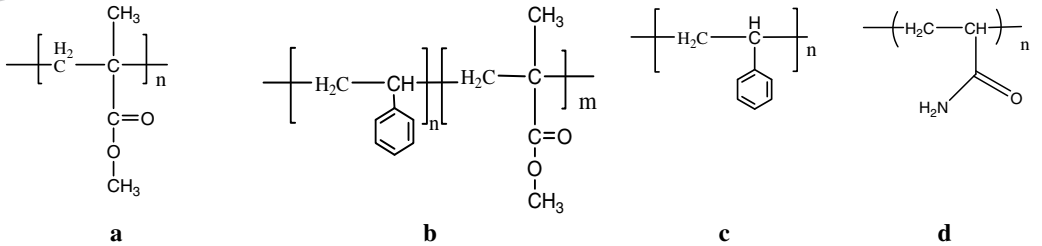

Figure 1. The chemical representations of outer and inner layer materials **(a)** PMMA **(b)** poly(methyl methacrylate-co-styrene) **(c)** PS and **(d)** PAAm

2.3. *Solvent selection and design*

Solvents and solvent systems are selected based on Hansen solubility parameters (HSP) using tabulated interactions of molecules in the form of polar (δ_p), dispersive (δ_d), and hydrogen bonding (δ_h) components [18]. Two-dimensional graphical representation of these parameters for our system is produced by combining the polar (δ_p) and dispersive (δ_d) components into a new parameter of $\delta_v = (\delta_d^2 + \delta_p^2)^{1/2}$ which is plotted against δ_h. Solvents for outer layer polymers are selected from among those located inside the solubility circle of each polymer considering the electrospinning properties of the polymeric solutions such as electrical conductivity and vapor pressure since these parameters are known to alter the borders of solubility area. Good and poor solvents for several polymers can be predicted by drawing a solubility circle defined by the Hansen coordinates and the radius of interaction [19]. On the other hand, PAAm as an inner layer material is mainly soluble in water, but different co-solvents with various volume ratios can be utilized to tailor the interaction of outer and inner layer solutions. The Hansen solubility parameter of solvent mixtures is calculated using $\delta_n^{Mix} = \sum a_i \delta_n^i$ equation where n represents the parameter type (p, d, or h) and a_i is the volume fraction of solvent i. After the selection of ideal solvents for electrospinning, polymer solutions with the unit of weight percentages (w/w) are prepared by appropriate amount of polymer and solvent, and stirred for 24 h at ambient temperature and pressure to obtain homogeneous solutions.

2.4. *Single and multi-axial electrospinning*

Electrospinning process is performed at ambient room conditions using multi-axial electrospinning set-up purchased from *Y*flow Company with a custom-made tri-axial nozzle. Hollow fibers covered by two different polymeric layers are produced by tri-axial electrospinning process given in Figure 2a. Also, the hollowness of fiber is also monitored by the formation of Taylor cone at the end of the syringe seen in Figure 2b.

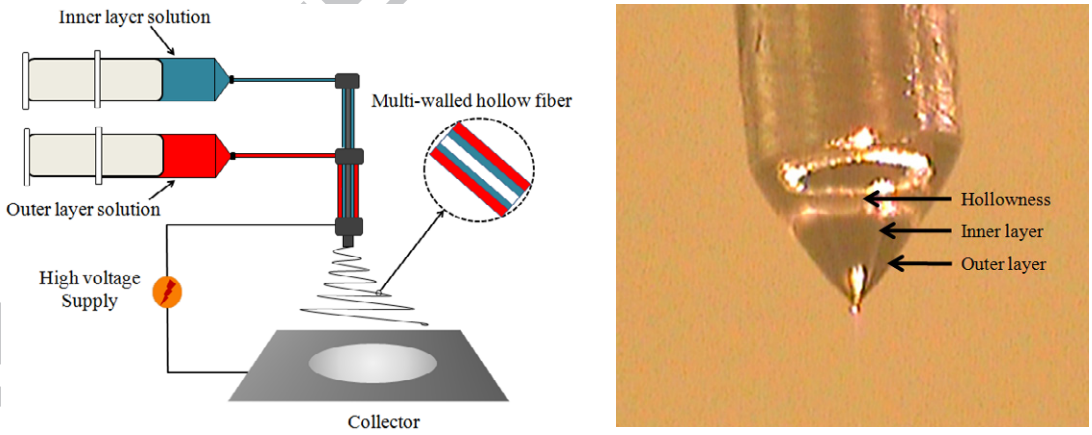

Figure 2. (a) Schematic representation of tri-axial electrospinning set-up (**b**) the high-speed camera image of Taylor cone composed of PMMA as an outer layer and PAAm as a middle layer.

All the fibers were electrospun with a nozzle to collector distance of 7 cm by tuning the applied voltage in the range of 5 kV to 30 kV. The flow rates of outer and inner layer

solutions are individually controllable using separate pumps, and are of the values of 20 µl/min and 15 µl/min, respectively. Solutions prepared are loaded independently into the syringes which are connected to concentric nozzles, and the flow rate of each layer is controlled by separate pumps.

2.5. Characterization

The structure of synthesized polymer was investigated by 500 MHz Varian Inova ^{1}H-Nuclear Magnetic Resonance (NMR). The molecular weight and polydispersity index of outer layer polymers were determined by Viscotek-VE2001 gel permeation chromatography (GPC) in DMF. The functional groups of polymers and fibers were investigated by Netzsch Fourier Transform Infrared Spectroscopy (FTIR). Thermal behaviors of polymers and fibers were examined by Netzsch Thermal Gravimetric Analyzer (TGA) and Differential Scanning Calorimeter (DSC) by a 10°C/min scanning rate under nitrogen atmosphere. The surface morphologies of fibers were analyzed by a Leo Supra 35VP Field Emission Scanning Electron Microscope (SEM) and JEOL 2100 Lab6 High Resolution Transmission Electron Microscopy (TEM). Elemental analysis of fibers was performed by Energy-Dispersive X-Ray (EDX) analyzing system. Taylor cone shape images were taken by high-speed camera.

3. Results and Discussion

3.1. Layer materials of multi-walled hollow electrospun fibers

3.1.1. Outer layer materials

For the production of composite hollow fibers, as can be recalled the hydrophobic polymers as a protective outer layer of fibers were synthesized through free radical polymerization in solution medium. Here, it should be noted that it is critical to choose the hydrophobic polymers as an outer layer material to prevent the diffusion of layers during electrospinning thus providing the layered structure. In multi-axial electrospinning process, PMMA, PS and poly(methyl methacrylate-co-styrene) are used as outer layer polymers, and molecular weight (Mw), polydispersity index (PDI) and glass transition temperature (T_g) of these polymers are given in Table 1. A more detailed description of the experimental procedures can be found in the electronic supplementary information.

Table 1. Mw, PDI and T_g of outer layer polymers of electrospun fibers

Polymer	T_g (°C)	Mw (g/mole)	PDI
PMMA	123	326000	3.2
PS	103	313000	1.7
Poly(methyl methacrylate-co-styrene)	98	185000	1.7

3.1.2 Inner layer materials

In the inner part of composite hollow fibers, the polymers with the hydrophilic nature are chosen to get the desired fiber structure. PAAm as a water-soluble polymer is synthesized for an inner layer of multi-walled hollow fibers via dispersion polymerization and free radical initiator. Viscosity average molecular weight (Mv) of PAAm, measured by Mark–Houwink

method, is about 87000 g/mole. T_g of PAAm is around 189°C. A more detailed explanation of PAAm synthesis can also be found in the electronic supplementary information.

3.2. Selection of suitable solvent systems by Hansen solubility parameters

Figure 3 exhibits 2-dimensional solubility diagram of PMMA, and the suitable solvents for complete solubility of PMMA are located within the circled area. As stated previously, PAAm as an inner layer is mainly soluble in water; however, different co-solvents with various volume ratios are utilized to tailor the interaction of inner and outer layer solutions.

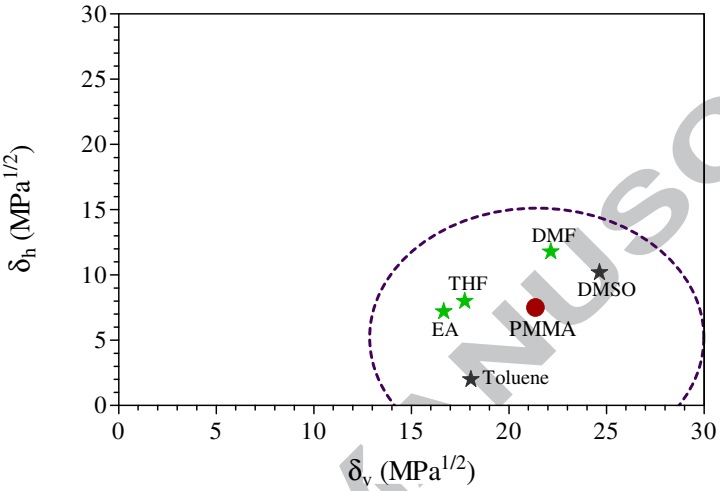

Figure 3. 2-dimensional solubility diagram of PMMA.

3.3. Study of layer materials by single electrospinning

Suitable window of processing and material parameters for stable electrospinning process of each polymer is initially determined by performing single-axial electrospinning. In the case of outer layer materials, polymer concentration in solution plays a critical role in final morphology of fibers. As such, the concentration of PMMA lower than 15 wt % leads to the formation of spherical particles while the concentration higher than 20 wt % results in uniform and brittle electrospun fibers as shown in Figure 4a. Such a difference in the form of final electrospun product is attributed to the increase in polymer chains in the solution, which enhances the entanglement density and raises the solution elastic behavior. It was observed that polymer concentration higher than 40 wt. %, is not suitable to produce uniform fibers. Single axial electrospinning conditions are also optimized for PAAm as a middle layer. PAAm nanofibers reveal the continuous, uniform and smooth morphology with an average diameter of 250 nm (see supp doc). Unlike fibers obtained using outer layer polymers, PAAm fibers do not show any brittleness and continuous fiber network is observed. Single axial electrospinning experiments show that optimum electrospinning parameters which render a stable Taylor cone and hence uniform fiber formation are those of solution concentration between 20 to 30 wt. %, deposition distance between 5-10 cm and the applied voltage between 5-20 kV.

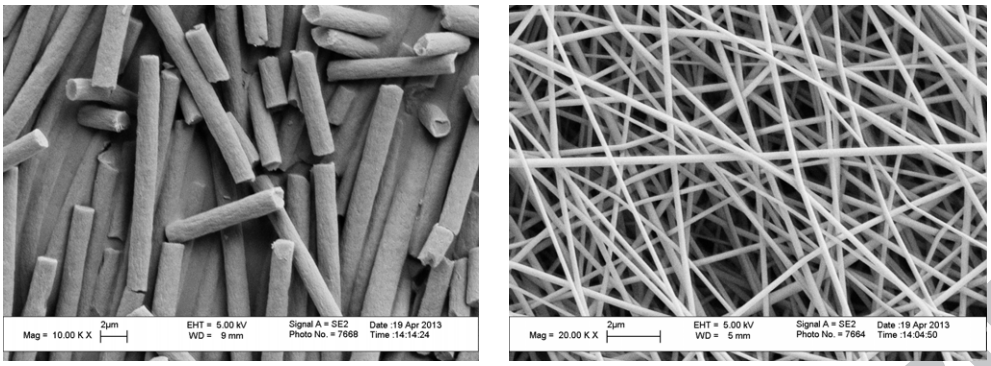

(a **(b**

Figure 4. SEM images of single axial electrospun fibers **(a)** PMMA and **(b)** PAAm. (The concentration of each polymeric solution is 30 wt. %).

3.4. Multi-walled hollow fibers by tri-axial electrospinning

3.4.1 The effect of solvent on the formation of multi-walled hollow fibers

The type of solvent is one of the most important and influential parameters in controlling the morphology and diameter of electrospun polymeric fibers [20]. Multi-axial electrospinning as a newly emerged technique for the fabrication of electrospun fibers with intricate and advanced morphology requires further considerations for the selection of proper solvent to obtain the desired fiber structures. Figure 5 gives SEM images for multi-walled hollow electrospun fibers with outer layer of PMMA and inner layer of PAAm by using different solvents in outer layer solution. The results show that the fiber diameter increases upon increasing solvent vapor pressure. DMF results in the formation of fiber with the diameter less than 100 nm whereas ethyl acetate (EA) increases the fiber diameter up to 500 nm, and the largest fiber diameter about 1 µm is obtained by THF. The high vapor pressure of THF provides faster drying of outer layer solution during electrospinning process, but solvents with lower vapor pressure like DMF bring about the longer drying time. Thus, polymeric jet with solvents of lower vapor pressure is exposed to instabilities for longer duration and in turn the diameter of fibers is reduced before reaching the surface of the collector. In addition, higher dielectric constant of solvent like DMF provides higher stored electrical energy, ion disassociation and free charge in solution jet. Hence, the polymeric jet is being subjected to higher electrical forces, thereby contributing to further reduction in fibers' diameter [21]. In addition, the inset image in Figure 5b indicates complete breakage of outer layer and the rupture of inner layer that reveals distinct layers and the hollowness of the fiber.

Figure 5 also indicates that the solvent type directly affects the surface morphology and porosity of the fibers. In the electrospinning process, rapid acceleration of jet toward the collector surface increases the surface area of the jet hence leading to significantly higher rate of solvent evaporation and rapid evaporation cooling. Thermodynamic instability caused by this cooling leads to phase separation of jet solution into the polymer-rich and solvent reach phase which after drying of the fibers the polymer rich phase remains and the solvent-rich phase forms pores [22]. Heat of vaporization in DMF is higher than THF, but higher rate of evaporation and lower heat capacity of THF made evaporation cooling phenomena stronger resulting in greater phase separation and more porosity within the final fibers. Furthermore, evaporation cooling during the electrospinning caused the condensation of water vapor in the

air onto the fiber surface as droplets known as “breath figures” left the pore on the fiber surface after drying of fibers [23].

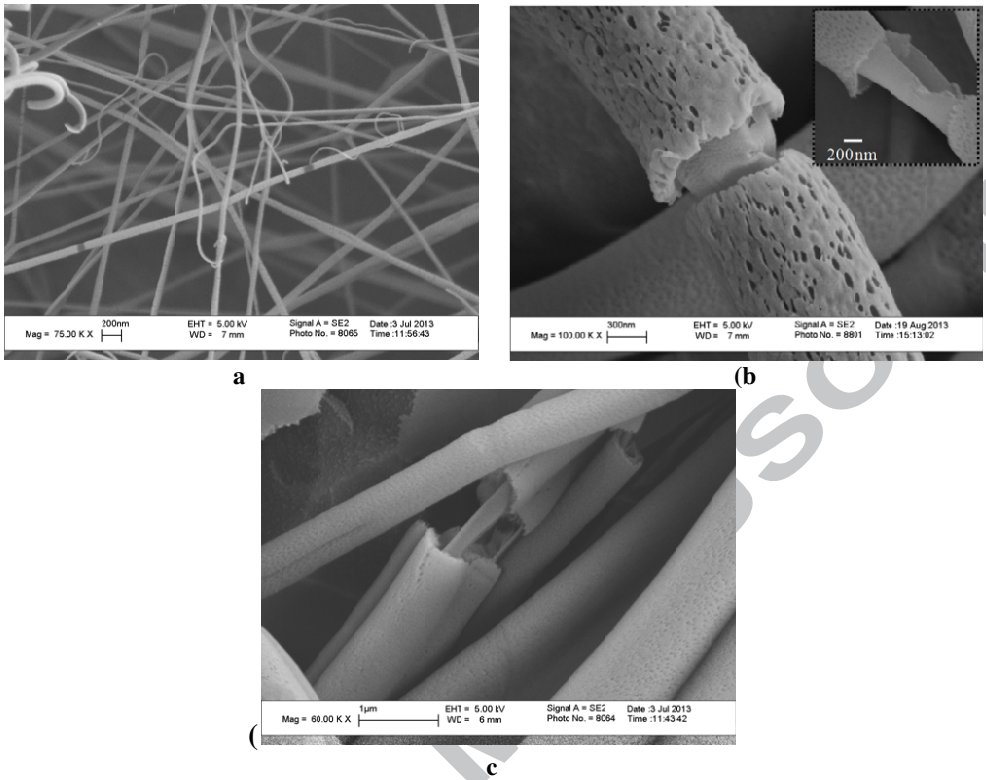

Figure 5. SEM images of electrospun multi-walled hollow PMMA/PAAm fibers fabricated by different outer wall solvents **(a)** DMF, **(b)** EA and **(c)** THF.

The miscibility of layer solutions in multi-axial electrospinning process is another parameter influencing the final morphology of fibers. It is expected that solutions with lower affinity with respect to one another form distinct layers with clear interface upon the electrospinning whereas solutions with partial miscibility causes diffusive interface morphology between the layers [19]. For instance, PS as an outer layer is completely soluble in DMF and PAAm is dissolved in water easily. During the process of these materials, water and DMF mixture with volume ratio of 3:2 (WD32) is used to dissolve PAAm inner layer but DMF present in both inner and outer layers increases the affinity of both inner and outer layer solutions whereby layers start to diffuse through each other. To explain the affinity of solutions in question quantitatively, it is prudent to refer to Hansen solubility space. In Figure 6, one can see that the WD32 solvent is located at a distance of 12.25 $MPa^{1/2}$ from DMF in Hansen space (high affinity) while water is at a longer distance of 30.6 $MPa^{1/2}$ from the WD32, implying less affinity to outer layer solution. SEM images in Figure 7 reveal the formation of electrospun multi-walled hollow fibers produced by different pairs of solutions providing different affinities for layers. Figure 7a shows a sharp and smooth interface between inner and outer layers of the fibers prepared by PAAm in water as an inner layer and PS in DMF as an outer layer. On the other hand, this distinction between layer materials is not observed in Figure 7b due to high affinity of layer solvents. One may note that the inner diameter of the severed surface shown in the inset of figure 7a is larger than the diameter of the stretched inner layer in the corresponding figure, hence pointing to the hollowness of the fiber.

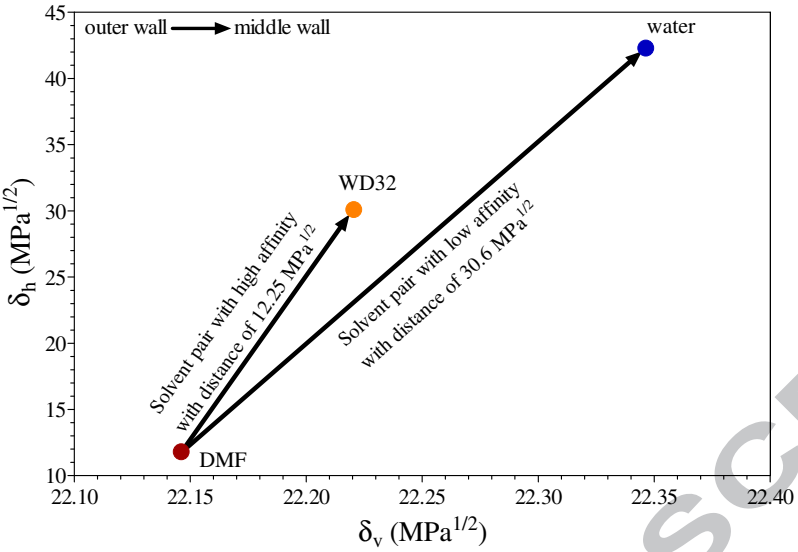

Figure 6. The graph of distance of inner layer solvent and outer layer solvent calculated by Hansen solubility space as an index of their affinity.

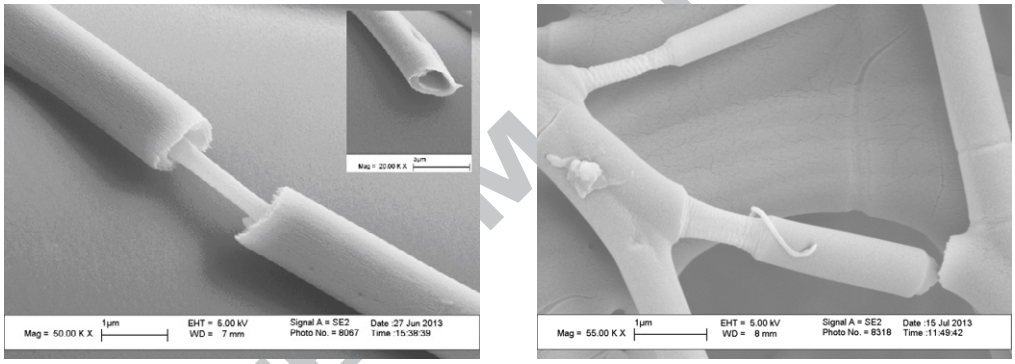

a **(b**

Figure 7. SEM images of multi-walled hollow electrospun fibers of PS/PAAm synthesized with the outer layer solvent of DMF by changing inner layer solvent of **(a)** water and **(b)** mixture of water/DMF (volume ratio 3:2).

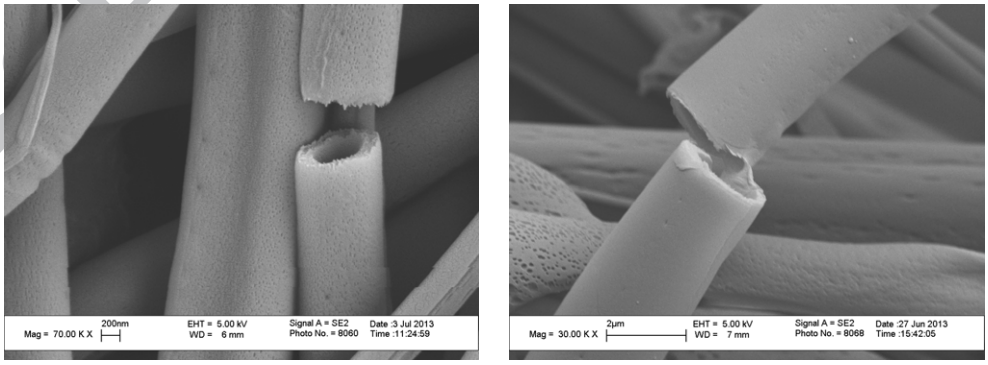

a **b**

Figure 8. SEM images of multi-walled hollow electrospun fibers of PS/PAAm synthesized with solvents of THF and water for the outer and inner layers, respectively: (a) and (b) present images at different magnifications.

For better visualization of the hollowness in the multi-walled hollow electrospun fibers, in Figure 8 are given SEM images of PS/PAAm fiber synthesized with solvents of THF and water for the outer and inner layers, respectively. Recalling that as the vapor pressure of the solvent increases, so does the diameter of the fiber, and hence, the hollowness can be easily noticed through paying attention to the topology of the fractured fiber surfaces.

3.4.2. The effect of applied voltage on the formation of multi-walled hollow fibers

Electrical field generated by applied voltage between nozzle and collector is another crucial factor for the production of hollow electrospun fibers. The polymer droplet on the tip of the nozzle needs applied voltage higher than threshold voltage, at which the electric force overcomes the forces associated with the surface tension letting jet to travel toward the collector surface [24]. The balance between the surface and electrical force is also critical in the shape of Taylor cone. Figure 9 represents the Taylor cone formations in different applied voltage. Unstable Taylor cone initiates at the applied voltage of 10 kV for PMMA/PAAm hollow fibers jet and then stable Taylor cone is monitored by increasing the voltage up to 20 kV. Moreover, it is observed that further increasing the applied voltage reduces the volume of the cone, and at the 30 kV, multiple cones are formed resulting in unstable and unpredictable electrospinning process. Figure 10 shows the graph of fiber diameter change as a function of applied voltage. As the applied voltage increases from 10 to 20 kV during the fabrication of hollow fibers with outer layer of PMMA solution in DMF and inner layer of PAAm solution in water/DMF mixture, it is observed that the fiber diameter also gradually increases. This can be attributed to the fact that since the applied voltage decreases the travel time of the fiber between the nozzle and collector thereby decreasing bending instabilities, and whipping motions of the fiber experience, the decrease in exposure time to these instabilities leads to increase in the fiber diameter with the increasing applied voltage. Moreover, increasing the applied voltage accelerates the electrospinning process but limits the fiber drying time before reaching the collector whereby wet fibers are gathered on the collector surface.

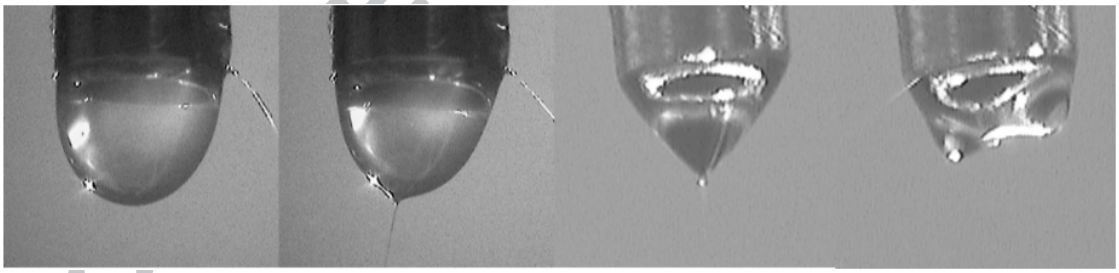

Figure 9. Taylor cone formation of PMMA 20 wt.% in EA as outer layer solution and PAAm in water as inner layer solution in different applied voltage **(a)** no voltage, **(b)** 10 kV, **(c)** 20 kV and **(d)** 30 kV.

Another important parameter affecting the formation of stable cone shape is the flow rate. It is known that if the flow rate of inner and outer layer solutions through the nozzles are insufficient to eject the solutions continuously from the tip of the nozzle, flow instabilities unavoidably occurs hence resulting in bead formation, or defects in the fiber structure [25]. Incompatibility in flow rates for inner and outer fluids can lead to non-uniformities in fiber layers. In course of determining the range of workable flow rates for inner and outer layer solutions, namely 10-50 µl/min, it is observed the best possible cone shape for core-shell formation is obtained by the flow rates of 20 µl/min and 15 µl/min for outer and inner layers,

respectively. In the electrospinning of multi-layer fibers, the flow rate of outer layer solution should be always higher than those of inner layer and core (if exists) solutions to have a complete coverage of these materials and in turn produce structures with uniform layers.

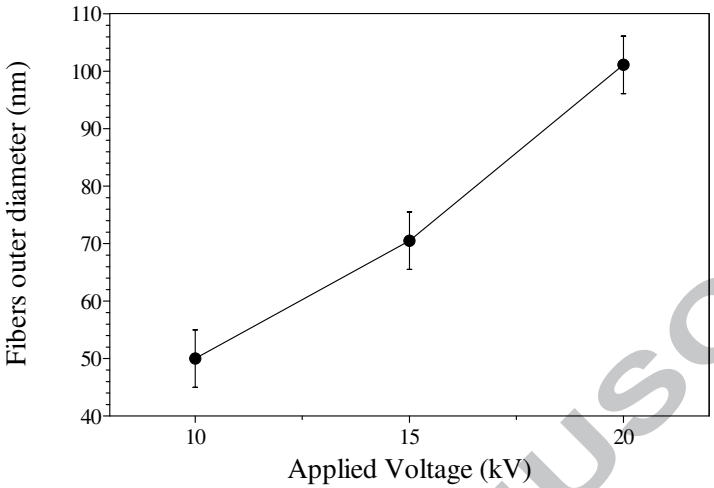

Figure 10. Changes in the fiber diameter by increasing the applied voltage for fibers with outer layer of PMMA in DMF and inner layer of PAAm in WD32 (water: DMF=3:2 (v/v)).

3.5.3 The effect of outer layer polymer on fiber formation and hollowness

In conventional core-shell electrospinning, it is a difficult process to control the hollowness continuously since the instabilities in the course of core formation can occur throughout the spinning process [26]. In this work, we have shown that the utilization of an inner layer, which is readily possible with tri-axial electrospinning process, can overcome these instabilities by acting as a barrier and increasing interconnection between layers. In order to be able to show that the hollowness and structural integrity of the fibers can be controlled, we have electrospun fibers using two different outer layer polymers, namely PMMA and PS while keeping the inner layer material the same, PAAm. Figure 11a and 11b show TEM images of tri-axial PMMA/PAAm hollow fibers. Bright sections in the central part of fibers with a diameter of about 100−125 nm correspond to hollow core formation. The inner layer of the fiber appears black in color whereas dark gray region belongs to the outer layer of fiber. In Figure 11c is given the rupture of inner layer observed in multi-walled hollow fiber structure. Figure 12 shows that the usage of PS as an outer layer instead of PMMA leads to an increase in the inner diameter up to 250 nm. One may reliably conclude from the presented TEM results that the diameter of hollowness can be adjusted by changing the type of polymer in the outer layer. Different polymers have dissimilar affinities with the same solvent, which can influence the drying behavior of solvents during the electrospinning process thereby affecting the wall thickness of the fibers and in turn their hollowness. The controllability of hollowness diameter can provide an easy encapsulation of functional materials with different viscosities if required, and increase the life-time of encapsulated materials through circumventing leakage.

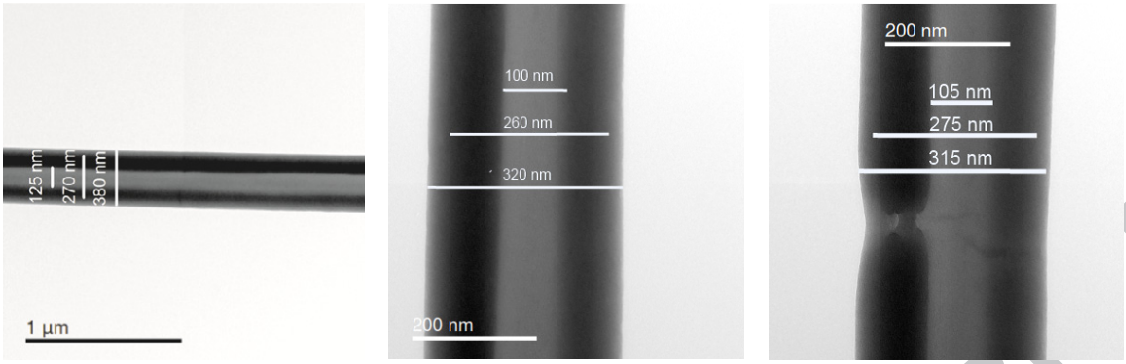

Figure 11. TEM images of **(a)** and **(b)** PMMA/PAAm multi-walled hollow fibers with continuous core structure at different magnifications, and **(c)** the rupture of middle layer in tri-axial hollow fiber structure (Outer layer solvent: EA, inner layer solvent: water).

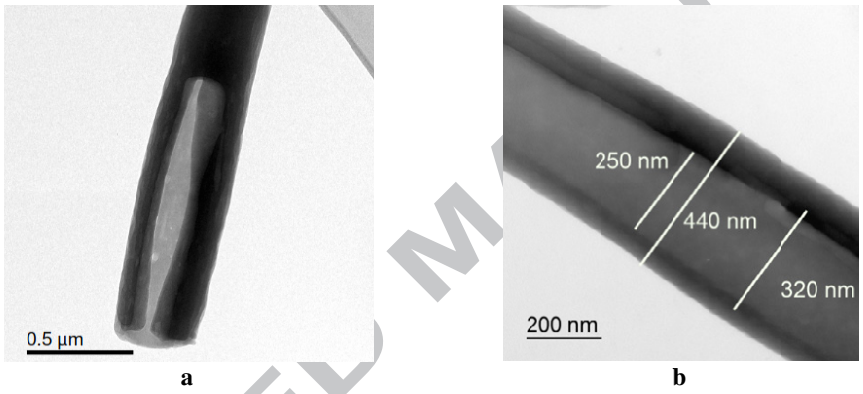

Figure 12. TEM images **(a)** and **(b)** of PS/PAAm hollow fibers in different regions and at different magnifications (Outer layer solvent: EA, inner layer solvent: water).

In addition to homopolymers, copolymers of styrene and methyl methacrylate are also utilized as an outer layer. Figure 13 shows SEM images of tri-axial hollow electrospun fibers fabricated by electrospinning of poly(methyl methacrylate-co-styrene) as an outer layer in different solvents, namely, EA, and THF. The layers of these hollow fibers produced by EA separate easily from each other and the proper connection is not achieved between inner and outer layers (Figure 13a). On the other hand, outer layer processed by THF is not easily separated from the inner layer and fiber elongation can be seen clearly in Figure 13b and 13c. Consequently, it is possible to fabricate electrospun hollow fibers with different structures and functionalities by using several polymers through tri-axial electrospinning technology.

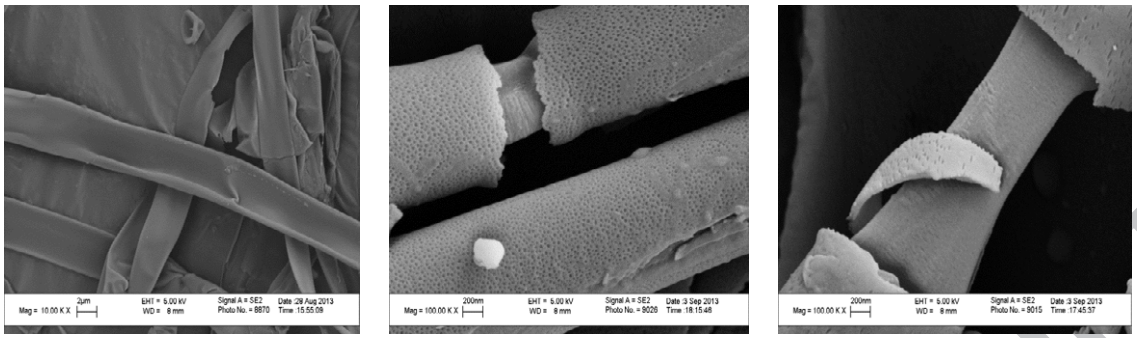

a **b** **c**

Figure 13. SEM images of multi-walled hollow fibers with PAAm as an inner layer and poly(methyl methacrylate-co-styrene) as an outer layer prepared by using solvent of **(a)** EA, **(b)** and **(c)** THF.

3.5. Structural and thermal analyses of multi-walled hollow fibers

The formation of tri-axial hollow fibers was also investigated by monitoring the functional groups of each layer. Figure 14 exhibits FTIR spectrum of multi-walled hollow fiber with PMMA as an outer layer and PAAm as an inner layer. For PMMA polymer, absorption bands at 2950 cm^{-1} and 1745 cm^{-1} indicate C-H and C=O stretchings, respectively [27]. For PAAm polymer, asymmetric and symmetric NH stretching of NH_2 contribute to absorption bands at around 3300 cm^{-1} [28]. EDX results showed that tri-axial hollow fiber included 56% carbon, 30% oxygen and 14% nitrogen. The nitrogen content in the fiber indicates the presence of PAAm in fiber structure.

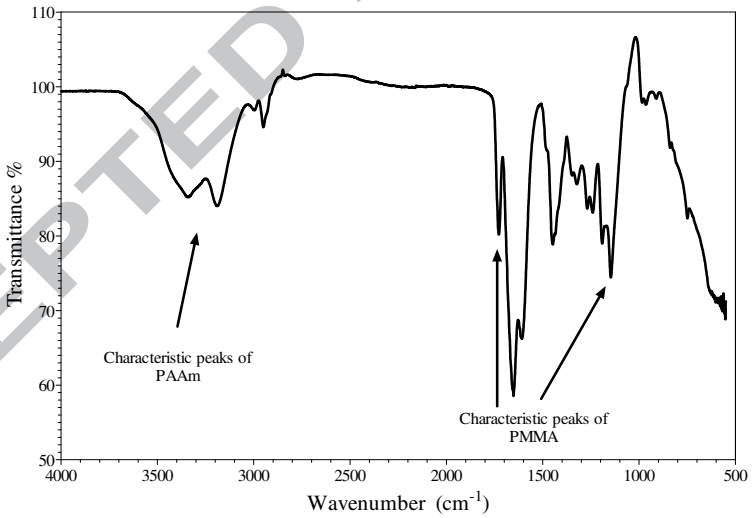

Figure 14. FTIR spectrum of multi-walled hollow electrospun fiber with PMMA as an outer layer and PAAm as an inner layer.

The thermal stabilities of PMMA/PAAm multi-walled hollow fibers were evaluated by means of TGA and DTA thermograms. Figure 15 exhibits TGA and DTA curves of PMMA and PAAm polymers and multi-walled hollow fiber. Neat radically prepared PMMA shows three steps of weight loss. At first step, PMMA lost 4 % of its weight between 175-225°C due to chain scissioning of head-to-head unstable and sterically hindered linkages [29]. The second stage of degradation with weight loss of 34% was observed between 250-325°C due

to scissioning of unsaturated ends (resulting from termination by disproportionation). In the last step, 62% of polymer weight were lost between 325-450°C described by random scissioning within the polymer chain [30]. In the case of neat PAAm, two stages of degradation were observed with 18% weight loss between 225-350°C because of amide side-groups decomposition and, 56% weight loss in the range of 350-500°C due to backbone decomposition [31]. The weight loss curve of multi-walled hollow fibers appeared between PMMA and PAAm (Figure 15a). As a result, FTIR and TGA analyses proved the successful formation of multi-walled hollow fibers with different layer polymers during tri-axial electrospinning process.

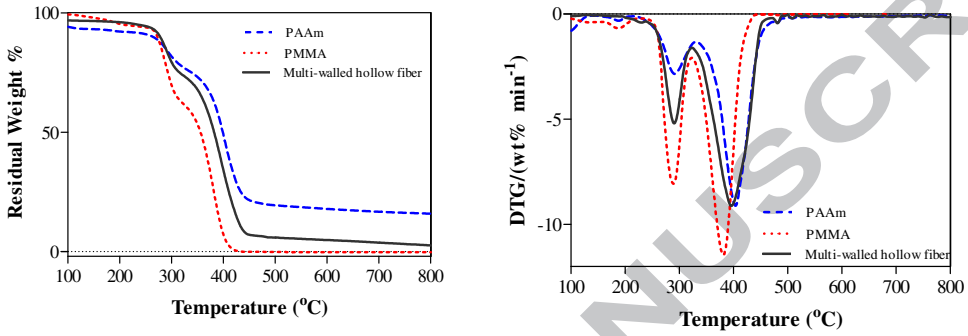

Figure 15. (a) TGA curves of PMMA, PAAm and multi-walled hollow fibers and **(b)** differential thermal analyses of PMMA, PAAm and multi-walled hollow fibers.

4. Conclusions

In the present work, multi-walled electrospun fibers with controllable hollowness and different polymeric layers were fabricated by a single step process. The inner and outer diameters of fibers and surface morphologies are controlled by changing the solvent type, applied voltage, polymer concentration and polymer type. The suitable window of material and processing parameters for electrospinning of each polymer were determined using single axial electrospinning. This was the first work in the literature to show the production of multi-walled hollow electrospun fibers covered by two different polymeric layers. The system and process parameters of tri-axial electrospinning were optimized to fabricate an ideal hollow structure. The diffusion of layers during electrospinning was controlled by using Hansen solvent selection methods. If the polymer concentration was lower than 15%, the sphere-based structure formation was observed. On the other hand, smooth fibers formation was monitored by increasing the polymer concentration. The porosity of fiber surface and the diameter of hollowness were directly affected by changing outer layer material and the solvent type. In conclusion, these novel fibers with different functionalities can be utilized in water filtration, composites, dialysis membranes, catalysis, drug delivery, membrane, photonics and coatings.

Acknowledgment

The authors gratefully acknowledge financial support from the Scientific and Technical Research Council of Turkey (TUBITAK) Project No: 112M312/COST MP1202 HINT project and thank to ESTEEM2 project for TEM characterization.

References:

[1] Müller GFJ, Stürzel M, Mülhaupt R. Core/Shell and Hollow Ultra High Molecular Weight Polyethylene Nanofibers and Nanoporous Polyethylene Prepared by Mesoscopic Shape Replication Catalysis. Advanced Functional Materials. 2014;24(19):2860–2864.
[2] Hong Y, Chen X, Jing X, Fan H, Gu Z, Zhang X. Fabrication and Drug Delivery of Ultrathin Mesoporous Bioactive Glass Hollow Fibers. Adv Funct Mater. 2010;20(9):1503-1510.
[3] Ou K-L, Chen C-S, Lin L-H, Lu J-C, Shu Y-C, Tseng W-C, et al. Membranes of epitaxial-like packed, super aligned electrospun micron hollow poly(l-lactic acid) (PLLA) fibers. Eur Polym J. 2011;47(5):882-892.
[4] Niu L, Zhao C-L, Kang J, Jin S, Guo J, Wei H. A chemical vapor sensor based on Rayleigh scattering effect in simplified hollow-core photonic crystal fibers. Opt Commun. 2014;313(15):243-247.
[5] Bognitzki M, Hou H, Ishaque M, Frese T, Hellwig M, Schwarte C, et al. Polymer, Metal, and Hybrid Nano- and Mesotubes by Coating Degradable Polymer Template Fibers (TUFT Process). Adv Mater (Weinheim, Ger). 2000;12(9):637-640.
[6] Qiu Y, Yu J. Synthesis of titanium dioxide nanotubes from electrospun fiber templates. Solid State Commun. 2008;148(11-12):556-558.
[7] Huang Z, Chen Y, Zhou W, Nie H, Hu Y. Preparation of silica hollow fibers by surface-initiated atom transfer radical polymerization from electrospun fiber templates. Mater Lett. 2009;63(21):1803-1806.
[8] Liu P, Zhu Y, Ma J, Yang S, Gong J, Xu J. Preparation of continuous porous alumina nanofibers with hollow structure by single capillary electrospinning. Colloids Surf, A. 2013;436:489–494.
[9] Li D, Xia Y. Direct Fabrication of Composite and Ceramic Hollow Nanofibers by Electrospinning. Nano Lett. 2004;4(5):933-938.
[10] Li D, McCann JT, Xia Y. Use of electrospinning to directly fabricate hollow nanofibers with functionalized inner and outer surfaces. Small. 2005;1(1):83-86.
[11] Zussman E, Yarin AL, Bazilevsky AV, Avrahami R, Feldman M. Electrospun Polyaniline/Poly(methyl methacrylate)-Derived Turbostratic Carbon Micro-/Nanotubes. Adv Mater. 2006;18(3):348-353.
[12] Dror Y, Salalha W, Avrahami R, Zussman E, Yarin AL, Dersch R, et al. One-step production of polymeric microtubes by co-electrospinning. Small. 2007;3(6):1064-1073.
[13] Ozden-Yenigun E, Simsek E, Menceloglu YZ, Atilgan C. Molecular basis for solvent dependent morphologies observed on electrosprayed surfaces. Physical Chemistry Chemical Physics. 2013;15:17862-17872.
[14] Kalra V, Lee JH, Park JH, Marquez M, Joo YL. Confined Assembly of Asymmetric Block-Copolymer Nanofibers via Multiaxial Jet Electrospinning. Small. 2009;5(20):2323–2332.
[15] Chen H, Wang N, Di J, Zhao Y, Song Y, Jiang L. Nanowire-in-Microtube Structured Core/Shell Fibers via Multifluidic Coaxial Electrospinning. Langmuir. 2010;26(13):11291–11296.
[16] Liu W, Ni C, Chase DB, Rabolt JF. Preparation of Multilayer Biodegradable Nanofibers by Triaxial Electrospinning. ACS Macro Letters. 2013;2(6):466–468.
[17] Han D, Steckl AJ. Triaxial electrospun nanofiber membranes for controlled dual release of functional molecules. ACS applied materials & interfaces. 2013;5(16):8241-8245.
[18] Hansen CM. Hansen Solubility Parameters: A User's Handbook: CRC Press LLC; 2000.
[19] Kurban Z, Lovell A, Bennington SM, Jenkins DWK, Ryan KR, Jones MO, et al. A Solution Selection Model for Coaxial Electrospinning and Its Application to Nanostructured

Hydrogen Storage Materials. The Journal of Physical Chemistry C. 2010;114(49):21201–21213.
[20] Luo CJ, Stride E, Edirisinghe M. Mapping the Influence of Solubility and Dielectric Constant on Electrospinning Polycaprolactone Solutions. Macromolecules. 2012;45(11):4669-4680.
[21] Zhou Q, Bao M, Yuan H, Zhao S, Dong W, Zhang Y. Implication of stable jet length in electrospinning for collecting well-aligned ultrafine PLLA fibers. Polymer. 2013;54(25):6867–6876.
[22] Luo CJ, Nangrejo M, Edirisinghe M. A novel method of selecting solvents for polymer electrospinning. Polymer. 2010;51(7):1654-1662.
[23] Megelski S, Stephens JS, Chase DB, Rabolt JF. Micro- and Nanostructured Surface Morphology on Electrospun Polymer Fibers. Macromolecules. 2002;35(22):8456-8466.
[24] Rahmat A, Tofighi N, Shadloo MS, Yildiz M. Numerical simulation of wall bounded and electrically excited Rayleigh–Taylor instability using incompressible smoothed particle hydrodynamics. Colloids and Surfaces A: Physicochemical and Engineering Aspects. 2014;In Press, Corrected Proof — Note to users.
[25] Sill TJ, von Recum HA. Electrospinning: Applications in drug delivery and tissue engineering. Biomaterials. 2008;29(13):1989-2006.
[26] McCann JT, Lia D, Xia Y. Electrospinning of nanofibers with core-sheath, hollow, or porous structures. J Mater Chem. 2005;15:735-738.
[27] Kaniappan K, Latha S. Certain Investigations on the Formulation and Characterization of Polystyrene / Poly(methyl methacrylate) Blends. International Journal of ChemTech Research. 2011;3(2):708-717.
[28] Murugan R, Mohan S, Bigotto A. FTIR and Polarised Raman Spectra of Acrylamide and Polyacrylamide. Journal of the Korean Physical Society. 1998;32(4):505-512.
[29] Kashiwagi T, Inaba A, Brown JE, Hatada K, Kitayama T, Masuda E. Effects of weak linkages on the thermal and oxidative degradation of poly(methyl methacrylates). Macromolecules. 1986;19(8):2160-2168.
[30] Ferriol M, Gentilhomme A, Cochez M, Oget N, Mieloszynski JL. Thermal degradation of poly(methyl methacrylate) (PMMA): modelling of DTG and TG curves. Polym Degrad Stab. 2003;79(2):271-281.
[31] Saeidi A, Katbab AA, Vasheghani-Farahani E, Afshar F. Formulation design, optimization, characterization and swelling behaviour of a cationic superabsorbent based on a copolymer of[3-(methacryloylamino)propyl]trimethylammonium chloride and acrylamide. Polym Int. 2004;53(1):92-100.

Graphical abstract

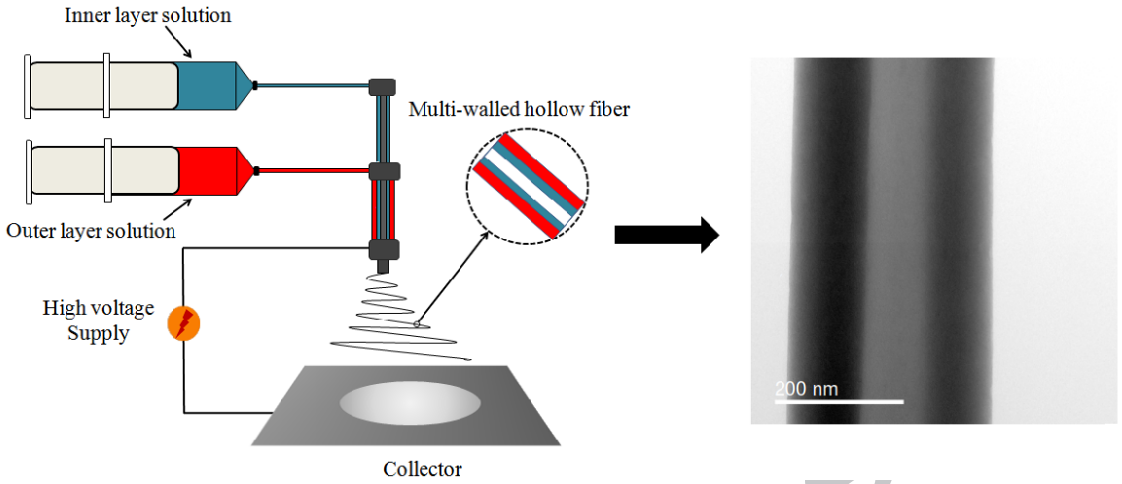

Highlights

- Multi-walled hollow fibers with a novel architecture are fabricated.
- The suitable window of material and processing parameters is presented.
- The inner and outer diameters of fibers and surface morphologies are controlled.